# Vacuum Polarization Energy for General Backgrounds in One Space Dimension

H. Weigel

Physics Department, Stellenbosch University, Matieland 7602, South Africa

For field theories in one time and one space dimensions we propose an efficient method to compute the vacuum polarization energy of static field configurations that do not allow a decomposition into symmetric and anti–symmetric channels. The method also applies to scenarios in which the masses of the quantum fluctuations at positive and negative spatial infinity are different. As an example we compute the vacuum polarization energy of the kink soliton in the  $\phi^6$  model. We link the dependence of this energy on the position of the soliton to the different masses.

#### I. INTRODUCTION

Vacuum polarization energies (VPE) sum the shifts of zero point energies of quantum fluctuations that interact with a (classical) background potential. Spectral methods [1] have been very successful in computing VPEs particularly for background configurations with sufficient symmetry to facilitate a partial wave decomposition for the quantum fluctuations. In this approach scattering data parameterize Green functions from which the VPE is determined. In particular the imaginary part of the two-point Green function at coincident points, *i.e.* the density of states, is related to the phase shift of potential scattering [2]. Among other features, the success of the spectral methods draws from the direct implementation of background independent renormalization conditions by identifying the Born series for the scattering data with the expansion of the VPE in the strength of the potential. The ultra-violet divergences are contained in the latter and can be re-expressed as regularized Feynman diagrams. In renormalizable theories the divergences are balanced by counterterms whose coefficients are fully determined in the perturbative sector of the quantum theory in which the potential is zero.

For field theories in one space dimension the partial wave decomposition separates channels that are even or odd under spatial reflection. We propose a very efficient method, that in fact is based on the spectral methods, to numerically compute the VPE for configurations that evade a decomposition into parity even and odd channels. This is particularly interesting for field theories that contain classical soliton solutions connecting vacua in which the masses of the quantum fluctuations differ. A prime example is the  $\phi^6$  model. For this model some analytical results, in particular the scattering data for the quantum fluctuations, have been discussed a while ago in Refs. [3, 4]. However, a full calculation of the VPE has not yet been reported. A different approach, based on the heat kernel expansion with  $\zeta$ -function regularization [5, 6] has already been applied to this model [7]<sup>1</sup>. This approach requires an intricate formalism on top of which approximations (truncation of the expansion) are required. We will see that they become less accurate as the background becomes sharper. We also note that a similar problem involving distinct vacua occurs in scalar electrodynamics when computing the quantum tension of domain walls [11].

We briefly review the setting of the one-dimensional problem. The dynamics of the field  $\phi = \phi(t, x)$  is governed by the Lagrangian

$$\mathcal{L} = \frac{1}{2} \partial_{\mu} \phi \, \partial^{\mu} \phi - U(\phi) \,. \tag{1}$$

The self-interaction potential  $U(\phi)$  typically has distinct minima and there may exist several static soliton solutions that interlink between two such minima as  $x \to \pm \infty$ . We pick a specific soliton, say  $\phi_0(x)$  and consider small fluctuations about it

$$\phi(t,x) = \phi_0(x) + \eta(t,x). \tag{2}$$

Up to linear order, the field equation turns into a Klein-Gordon type equation

$$\left[\partial_{\mu}\partial^{\mu} + V(x)\right]\eta(t,x) = 0, \qquad (3)$$

where  $V(x) = U''(\phi_0(x))$  is the background potential generated by the soliton. At spatial infinity V(x) approaches a constant to be identified as the mass (squared) of the quantum fluctuations. In general, as e.g. for the  $\phi^6$  model with  $U(\phi) = \frac{\lambda}{2}\phi^2(\phi^2 - \Lambda^2)^2$ , we allow  $\lim_{x \to -\infty} V(x) \neq \lim_{x \to \infty} V(x)$ . This gives rise to different types of quantum

<sup>&</sup>lt;sup>1</sup> See Refs. [8–10] for reviews of heat kernel and  $\zeta$ -function methods.

fluctuations. While  $\phi_0$  is classical, the fluctuations are subject to canonical quantization so that the above harmonic approximation yields the leading quantum correction. As a consequence of the interaction with the background the zero point energies of all modes change and the (renormalized) sum of all these changes is the VPE, cf. Sec. III.

#### II. PHASE SHIFTS

As will be discussed in Sec. III the sum of the scattering (eigen)phase shifts is essential to compute the VPE from spectral methods. We extract scattering data from the stationary wave equation,  $\eta(t,x) \to e^{-iEt}\eta(x)$ ,

$$E^{2}\eta(x) = \left[-\partial_{x}^{2} + V(x)\right]\eta(x). \tag{4}$$

According to the above described scenario we define  $m_L^2 = \lim_{x \to -\infty} V(x)$  and  $m_R^2 = \lim_{x \to \infty} V(x)$  and take the convention  $m_L \le m_R$ , otherwise we just relabel  $x \to -x$ . We introduce a discontinuous pseudo potential

$$V_p(x) = V(x) - m_L^2 + (m_L^2 - m_R^2) \Theta(x_m)$$
(5)

with  $\Theta(x)$  being the step function. Any finite value may be chosen for the matching point  $x_m$ . In contrast to V(x),  $V_p(x) \to 0$  as  $x \to \pm \infty$ . Then the stationary wave equation, (4) reads

$$\left[-\partial_x^2 + V_p(x)\right] \eta(x) = \begin{cases} k^2 \eta(x), & \text{for } x \le x_m \\ q^2 \eta(x), & \text{for } x \ge x_m \end{cases}$$
 (6)

where  $k = \sqrt{E^2 - m_L^2}$  and  $q = \sqrt{E^2 - m_R^2} = \sqrt{k^2 + m_L^2 - m_R^2}$ . We emphasize that solving Eq. (6) is equivalent to solving Eq. (4). We factorize coefficient functions A(x) and B(x) appropriate for the scattering problem via  $\eta(x) = A(x)e^{ikx}$  for  $x \le x_m$  and  $\eta(x) = B(x)e^{iqx}$  for  $x \ge x_m$ :

$$A''(x) = -2ikA'(x) + V_p(x)A(x) \quad \text{and} \quad B''(x) = -2iqB'(x) + V_p(x)B(x),$$
 (7)

where a prime denotes a derivative with respect to x. In appendix B of Ref. [2] related functions,  $g_{\pm}(x)$  were introduced to parameterize the Jost solutions for imaginary momenta. The boundary conditions  $A(-\infty) = B(\infty) = 1$  and  $A'(-\infty) = B'(\infty) = 0$  yield the scattering matrix by matching the solutions at  $x = x_m$ . Above threshold,  $k \ge \sqrt{m_R^2 - m_L^2}$  so that q is real, the scattering matrix is

$$S(k) = \begin{pmatrix} e^{-iqx_m} & 0 \\ 0 & e^{ikx_m} \end{pmatrix} \begin{pmatrix} B & -A^* \\ iqB + B' & ikA^* - A'^* \end{pmatrix}^{-1} \begin{pmatrix} A & -B^* \\ ikA + A' & iqB^* - B'^* \end{pmatrix} \begin{pmatrix} e^{ikx_m} & 0 \\ 0 & e^{-iqx_m} \end{pmatrix}, \tag{8}$$

where  $A=A(x_m)$ , etc. are the coefficient functions at the matching point. Conventions are that the diagonal and off-diagonal elements of S contain the transmission and reflections coefficients, respectively [12]. Below threshold we parameterize for  $x \geq x_m$ :  $\eta(x) = B(x) e^{-\kappa x}$  with  $\kappa = \sqrt{m_R^2 - m_L^2 - k^2} \geq 0$  replacing -iq in Eq. (7) so that B(x) is real. Then

$$S(k) = -\frac{A(B'/B - \kappa - ik) - A'}{A^*(B'/B - \kappa + ik) - A'^*} e^{2ikx_m}$$
(9)

is the reflection coefficient. In both cases we compute the sum of the eigenphase shifts  $\delta(k) = -(i/2) \text{Indet} S(k)$ . The negative sign on the right hand side of Eq. (9) suggests that (in most cases)  $\delta(0)$  is an odd multiple of  $\frac{\pi}{2}$  in agreement with Levinson's theorem. When the scattering problem diagonalizes into symmetric (S) and anti-symmetric (A) channels and taking  $\delta(k) \to 0$  as  $k \to \infty$ , the theorem states that  $\delta_S(0) = \pi(n_S - \frac{1}{2})$  and  $\delta_A(0) = \pi n_A$ , where  $n_S$  and  $n_A$  count the bound states in the two channels [13, 14]. The additional  $-\pi/2$  in the symmetric channel arises because in that channel it is the derivative of the wave function that vanishes at x = 0, rather than the wave function itself. For scattering off a background that does not decompose into these channels we have  $\delta(0) = \pi(n - \frac{1}{2})$ , where n is the total number of bound states [12]. There are particular cases in which  $\delta(0)$  is indeed an integer multiple of  $\pi$ . Examples are reflectionless potentials and the case  $V(x) \equiv 0$ . Then there exist threshold states contributing  $\frac{1}{2}$  to n.

The step potential of hight  $m_R^2 - m_L^2$  centered at  $x = x_m$  corresponds to  $V_p \equiv 0$ . In this case the wave equation is solved by  $A(x) = B(x) \equiv 1$  and

$$\delta_{\text{step}}(k) = \begin{cases} (k-q)x_m, & \text{for } k \ge \sqrt{m_R^2 - m_L^2} \\ kx_m - \arctan\left(\frac{\sqrt{m_R^2 - m_L^2 - k^2}}{k}\right), & \text{for } k \le \sqrt{m_R^2 - m_L^2} \end{cases}$$

$$(10)$$

agrees with textbook results.

#### III. VACUUM POLARIZATION ENERGY

Formally the VPE is the sum of the shifts of the zero point energies due to the interaction with a background potential that is generated by the field configuration  $\phi_0$ ,

$$E_{\text{vac}}[\phi_0] = \frac{1}{2} \sum_j \left( E_j[\phi_0] - E_j^{(0)} \right) + E_{\text{ct}}[\phi_0]. \tag{11}$$

Regularization for this logarithmically divergent sum is understood. When combined with the counterterms,  $E_{\rm ct}$  a unique finite result arises after removing regularization. Typically there are two contributions in the sum of Eq. (11): (i) explicit bound and (ii) continuous scattering states. The latter part is obtained as an integral over one particle energies weighted by the change in the density of states,  $\Delta \rho(k)$ . We find the density  $\rho(k) = \frac{dN(k)}{dk}$  for scattering modes incident from negative infinity by discretizing  $kL + \delta(k) = N(k)\pi$  where  $\delta(k)$  is phase shift. Adopting the continuum limit  $L \to \infty$  and subtracting the result from the non-interacting case yields the Krein formula [15],

$$\Delta \rho(k) = \rho(k) - \rho^{(0)}(k) = \frac{1}{\pi} \frac{d}{dk} \delta(k). \tag{12}$$

The situation for modes incident from positive infinity is not as straightforward. Here we count levels (above threshold) by setting  $qL + \delta(k) = N(k)\pi$ . Since k is the label for the free states we get an additional contribution to the change in the density of states

$$\frac{L}{\pi} \frac{d}{dk} \left[ q - k \right] = \frac{L}{\pi} \left[ \frac{k}{\sqrt{k^2 + m_L^2 - m_R^2}} - 1 \right] = \frac{L}{\pi} \left[ \frac{\sqrt{E^2 - m_L^2}}{\sqrt{E^2 - m_R^2}} - 1 \right]. \tag{13}$$

Formally it adds a portion to the VPE that is not sensitive to the details of the potential. Its omission corresponds to the selection of a particular L independent part from the effective potential as e.g. in Eq. (3.42) of Ref. [11].

Then the VPE is solely extracted from the Krein formula. Integrating by parts and imposing the no–tadpole renormalization prescription yields

$$E_{\text{vac}} = \frac{1}{2} \sum_{j} (E_j - m_L) - \frac{1}{2\pi} \int_0^\infty dk \, \frac{k}{\sqrt{k^2 + m_L^2}} \left( \delta(k) - \delta^{(1)}(k) \right) \,. \tag{14}$$

The explicit sum runs over the discrete bound states that are obtained from the solutions to Eq. (4) that exponentially approach zero at spatial infinity. The subtraction under the integral refers to the Born approximation with respect to the potential  $V(x) - m_L^2$ . We stress that it does not refer to  $V_p(x)$  because the no–tadpole renormalization implements a counterterm that is local in the full potential. In general this disallows to write  $\delta^{(1)}(k) \sim -(1/2k) \int dx [V(x) - m_L^2]$ , because the Born approximation to the step potential cannot be written as this integral. Yet, its phase shift is well defined, Eq. (10) and the large momentum contribution, which is represented by the Born approximation, can easily be computed from Eq. (10)

$$\delta_{\text{step}}(k) \longrightarrow \frac{x_m}{2k} \left( m_R^2 - m_L^2 \right) \quad \text{as} \quad k \longrightarrow \infty.$$
 (15)

By definition, the Born approximation is linear in the potential. We use Eq. (5) to write  $V(x) - m_L^2 = V_p(x) + (m_R^2 - m_L^2) \Theta(x_m)$  and obtain the Born approximation

$$\delta^{(1)}(k) = -\frac{1}{2k} \int_{-\infty}^{\infty} dx \, V_p(x) \Big|_{x_m} + \frac{x_m}{2k} \left( m_R^2 - m_L^2 \right) = -\frac{1}{2k} \int_{-\infty}^{\infty} dx \, V_p(x) \Big|_{0}. \tag{16}$$

The subscript recalls that  $V_p(x)$  is defined with respect to a specific matching point  $x_m$ . However, the final Born approximation does not depend on  $x_m$ . This is a step towards establishing that the VPE does not depend on the matching point. We stress that this independence does not reflect translational invariance of the system as described by shifting the coordinate  $x \to x - x_0$  in V(x). On the contrary, Eq. (16) shows that at least the Born approximation varies under this transformation<sup>2</sup>.

<sup>&</sup>lt;sup>2</sup> It seems suggestive that the Born approximation should have a step function factor  $\Theta(k-\sqrt{m_R^2-m_L^2})$ . In the limit  $m_R \to m_L$  its modification of the VPE is proportional to  $\frac{x_m}{m_L}(m_R^2-m_L^2)^{3/2}$ . It is thus of higher order and also violates the  $x_m$  independence. Hence this factor is not part of the Born approximation.

When the potential is reflection symmetric the scattering problem separates into even and odd channels. This symmetry also implies q = k and allows to analytically continue to imaginary k = it with  $t \ge 0$  straightforwardly. Integrating over t collects the bound state contribution [1] and the VPE is

$$E_{\text{vac}}^{(S)} = \int_{m_L}^{\infty} \frac{dt}{2\pi} \frac{t}{\sqrt{t^2 - m_L^2}} \left[ \ln \left\{ g(t, 0) \left( g(t, 0) - \frac{1}{t} g'(t, 0) \right) \right\} \right]_1.$$
 (17)

Again the Born approximation has been subtracted as indicated by the subscript. Here g(t, x) is the non–trivial factor of the Jost solution on the imaginary axis that solves the DEQ

$$g''(t,x) = 2tg'(t,x) + V(x)g(t,x)$$
(18)

with the boundary condition  $g(t, \infty) = 1$  and  $g'(t, \infty) = 0$ .

Above we have used heuristic arguments to compute the VPE from scattering data. We stress that it can be derived from fundamental concepts of quantum field theory [2].

#### IV. NUMERICAL RESULTS

For simplicity we scale to dimensionless coordinates and fields such that as many as possible model parameters, for example  $\lambda$  and  $\Lambda$  from the introduction, are unity.

In all considered cases we have ensured that the phase shift does not vary with the choice of  $x_m$ ; that Levinson's theorem is reproduced; and that attaching flux factors  $S_{11} \to \sqrt{\frac{q}{k}} e^{i(q-k)x_m} S_{11}$  and  $S_{22} \to \sqrt{\frac{k}{q}} e^{i(k-q)x_m} S_{22}$  to the transmission coefficients always produces a unitary scattering matrix. When  $m_L = m_R$  we have also numerically verified that the sum of the eigenphase shifts equals the phase of the transmission coefficient  $S_{11} = S_{22}$  [16].

# A. Symmetric background

We first compare the result from the novel method for cases in which V(x) is reflection symmetric and the approach via Eq. (17) is applicable. Analytic results are available for the  $\phi^4$  kink and sine–Gordon models that have background potentials [as in Eq.(3)]

$$V_{\rm K}(x) = 6\tanh^2(x) - 2$$
 and  $V_{\rm SG}(x) = 8\tanh^2(2x) - 4$ , (19)

with  $m_L = m_R = 2$ . The numerical simulation for Eq. (14) agrees with the respective VPEs,  $E_{\text{vac,K}} = \sqrt{2}/4 - 3/\pi$  and  $E_{\text{vac,SG}} = -2/\pi$  [17], to better than one in a thousand.

We next compute the vacuum polarization energies of the  $U(\phi) = \frac{1}{2}(\phi^2 + a^2)(\phi^2 - 1)^2$  model, where a is a real parameter. For  $a \neq 0$  there is only a single soliton solution that interlinks the vacua<sup>3</sup>  $\phi_{\text{vac}} = \pm 1$  [3]:

$$\phi_0(x) = a \frac{X - 1}{\sqrt{4X + a^2 (1 + X)^2}}$$
 where  $X = e^{2\sqrt{1 + a^2} x}$ . (20)

For this model VPE results from a heat kernel calculation [5] are available. By comparing to our results, we estimate the validity of the approximations applied in the that approach. This comparison is essential because (to our knowledge) the only estimate of the VPE in the pure (a=0)  $\phi^6$  model, which is a main target of the present investigation, utilizes this technique [7]. The results are presented in table I and we observe that the various computations agree well for moderate and large a. The methods based on scattering data agree within numerical precision. But when a is small deviations of about 10-15% are observed for the (approximative) heat kernel method.

<sup>&</sup>lt;sup>3</sup> The potential  $U(\phi)$  has two global minima at  $\phi = \pm 1$  for  $a^2 > \frac{1}{2}$ . When  $a^2 < \frac{1}{2}$  a third (local) minimum exists. The three minima are degenerate for a = 0.

| a   | heat kernel, Ref. [5] | Jost, Eq. (17) | present, Eq. (14) |
|-----|-----------------------|----------------|-------------------|
| 0.1 | -1.349                | -1.461         | -1.462            |
| 0.2 | -1.239                | -1.298         | -1.297            |
| 1.0 | -1.101                | -1.100         | -1.102            |
| 1.5 | -1.293                | -1.295         | -1.297            |

TABLE I: Numerical VPEs for the symmetric background based on the soliton of the  $(\phi^2 + a^2)(\phi^2 - 1)^2$  model.

|                          |         |         |         |         |         |         | present, Eq. (14) |
|--------------------------|---------|---------|---------|---------|---------|---------|-------------------|
| $A = 2.5 , \sigma = 1.0$ | -0.0369 | -0.0324 | -0.0298 | -0.0294 | -0.0293 | -0.0292 | -0.0293           |
| D                        |         |         |         |         |         |         |                   |
| R                        | 4.0     | 5.0     | 6.0     | 7.0     | 8.0     | 9.0     | present, Eq. (14) |

TABLE II: Comparison of different methods to compute the VPE for a non–symmetric background. The R dependent data are half the VPE of the background, Eq. (21) computed via Eq. (17).

#### B. Asymmetric background, identical vacua

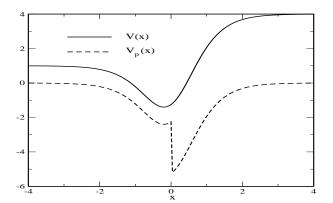
For the lack of a (simple) soliton model we consider the two parameter  $(A, \sigma)$  pseudo potential  $V_p(x) = Axe^{-x^2/\sigma^2}$ . The present method can be applied directly but also the standard spectral methods, Eq. (17) can employed after symmetrizing

$$V_R(x) = A \left[ (x+R)e^{-\frac{(x+R)^2}{\sigma^2}} - (x-R)e^{-\frac{(x-R)^2}{\sigma^2}} \right]$$
 (21)

so that the limit  $R \to \infty$  should give twice the VPE of  $V_p(x)$  [18]. Table II verifies that agreement is obtained, but large values for R are needed to avoid interference effects for wide background potentials.

# C. Asymmetric background, unequal vacua, $\phi^6$ model

We now turn to the pure  $\phi^6$  model with  $U(\phi) = \frac{1}{2}\phi^2 \left(\phi^2 - 1\right)^2$ . For a = 0 the soliton of Eq. (20) ceases to be a solution. However, there are solitons that interlink the degenerate vacua at  $\phi_{\rm vac} = 0$  and  $\phi_{\rm vac} = \pm 1$ . The curvatures of  $U(\phi)$  at these vacua differ so that the masses of the corresponding fluctuations are unequal. The soliton that corresponds to  $m_L = 1$  and  $m_R = 2$  is  $\phi_0(x) = \left(1 + {\rm e}^{-2x}\right)^{-1/2}$  [3]. The resulting potentials for the fluctuations are shown in the left panel of figure 1. Also shown is the resulting sum,  $\delta(k)$ , of the eigenphase shifts as obtained from the scattering matrix, Eqs. (8) and (9). The direct numerical calculation provides a discontinuous function between  $-\pi/2$  and  $\pi/2$ . The discontinuities are removed uniquely by adding appropriate multiples of  $\pi$  and demanding that



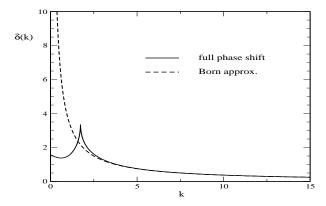


FIG. 1: Potentials (left panel) and phase shift (right panel) for scattering off a soliton in the  $\phi^6$  model. The pseudo potential  $V_p(x)$  is shown for  $x_m = 0$ .

|               |        |        |        |        |        | •      |
|---------------|--------|--------|--------|--------|--------|--------|
|               | 1.0    |        |        |        |        |        |
| $E_{\rm vac}$ | 0.1660 | 0.1478 | 0.1385 | 0.1363 | 0.1355 | 0.1355 |

TABLE III: VPEs for  $V_{\alpha}(x) = \frac{3}{2}[1 + \tanh(\alpha x)]$ . The entry 'step' refers to using  $\delta_{\text{step}}$  from Eq. (10) with  $x_m = 0$  in Eq. (14).

|              | $E_{ m vac}$ |       |        |        |                            |  |  |
|--------------|--------------|-------|--------|--------|----------------------------|--|--|
| $x_0$        | _            | -1    | -      | 1      | 2                          |  |  |
| $\phi^6$     | 0.154        | 0.053 | -0.047 | -0.148 | -0.249<br>-0.057<br>-0.064 |  |  |
| $\alpha = 2$ | 0.351        | 0.250 | 0.148  | 0.046  | -0.057                     |  |  |
| $\alpha = 5$ | 0.341        | 0.240 | 0.139  | 0.037  | -0.064                     |  |  |

TABLE IV: VPEs as a function of the center of the configurations mentioned in the text. The two entries  $\alpha = 2$  and  $\alpha = 5$  refer to the choices in  $\tanh[\alpha(x + x_0)]$ .

typical for threshold scattering, remains. Note also that  $\delta(0) = \frac{\pi}{2}$  complies with Levinson's theorem in one space dimension as there is only a single bound state: the translational zero mode of the soliton.

Our results for the momentum dependence of the phase shift (and reflection coefficient) agree with the formulas given in Refs. [3, 4] up to overall signs. We are confident about our signs from Levinson's theorem and the Born approximation. Putting things together we find the vacuum polarization energy of the kink in the  $\phi^6$  model

$$E_{\text{vac}} = -0.5 + 0.4531 = -0.0469, (22)$$

where the summands denote the bound state and (renormalized) continuum parts as separated in Eq. (14).

In Ref. [7] the VPE of the  $\phi^6$  model kink was estimated relative to  $V_{\alpha}(x) = \frac{3}{2} [1 + \tanh(\alpha x)]$  for  $\alpha = 1$ . In table III we give our results for various values of  $\alpha$ . For  $\alpha = 1$  our relative VPE is  $\Delta E_{\rm vac} = -0.0469 - 0.1660 = -0.2129$  to be compared with  $-0.1264\sqrt{2} = -0.1788$  from Ref. [7]. In view of the results shown in table I, especially for small a, these data match within the validity of the approximations applied in the heat kernel calculation.

#### D. Translational variance and symmetrization

We complete the discussion of the numerical results with a contemplation on translational invariance. In Sec. III we have already seen that the Born approximation changes when the center of the configuration is shifted by a finite amount. To investigate this further, we compute the VPE for the  $\phi^6$  kink  $\left[1 + \mathrm{e}^{-2(x+x_0)}\right]^{-1/2}$  in  $U''(\phi)$  and  $V(x) = \frac{3}{2} \mathrm{tanh}[\alpha(x+x_0)]$  as a generalization of the above study. The dependence on  $x_0$  originates solely from the phase shift part because bound states move with  $x_0$  without changing their energy eigenvalues. In Ref. [4] this  $x_0$  dependence was removed as part of the renormalization condition. This is not fully acceptable since the renormalization conditions should not depend on the field configuration.

For both potentials the numerical results from table IV show that the VPE decreases by about 0.101 per unit of shifting the center towards negative infinity. We can build up a similar scenario in form of a symmetric barrier  $V_{\rm SB}^{(x_0)}(x) = v_0 \Theta\left(\frac{x_0}{2} - |x|\right)$  whose VPE can be straightforwardly computed from Eq. (17). Substituting  $V_{\rm SB}^{(x_0)}$  into the DEQ, Eq. (18) yields

$$g(t,0) = \frac{\kappa_1 e^{-\kappa_2 x_0/2} - \kappa_2 e^{-\kappa_1 x_0/2}}{\kappa_1 - \kappa_2} \quad \text{and} \quad g'(t,0) = \frac{\kappa_1 \kappa_2}{\kappa_1 - \kappa_2} \left( e^{-\kappa_2 x_0/2} - e^{-\kappa_1 x_0/2} \right), \quad (23)$$

with  $\kappa_{1,2} = t \pm \sqrt{t^2 + v_0}$ . Since we only consider the barrier with  $v_0 > 0$ , the  $\kappa_{1,2}$  are always real. The relevant Born approximation is particularly simple

$$\ln \left\{ g(t,0) \left( g(t,0) - \frac{1}{t} g'(t,0) \right) \right\} = \frac{v_0 x_0}{2t} + \mathcal{O}\left(v_0^2\right) . \tag{24}$$

We these ingredients we have evaluated the integral in Eq. (17) using  $v_0 = m_R^2 - m_L^2 = 3$  as suggested by the  $\phi^6$  model kink and find

$$\lim_{x_0 \to \infty} \frac{E_{\text{vac}}[V_{\text{SB}}^{(x_0)}]}{x_0} \approx -0.1015.$$
 (25)

We can relate this result to the energy density of a step functuion potential at spatial infinity using the phase shift from Eq. (10)

$$\frac{E_{\text{vac}}[V_{\text{step}}^{(x_m)}]}{|x_m|} \to -\text{sign}(x_m) \left[ \int_0^{\sqrt{v_0}} \frac{dk}{4\pi} \frac{2k^2 - v_0}{\sqrt{k^2 + m_L^2}} + \int_{\sqrt{v_0}}^{\infty} \frac{dk}{4\pi} \frac{2k^2 - 2k\sqrt{k^2 - v_0} - v_0}{\sqrt{k^2 + m_L^2}} \right] \quad \text{as} \quad |x_m| \to \infty. \quad (26)$$

For  $m_L = 1$  and  $v_0 = 3$  the expression is square brackets has the numerical value -0.1013. These data suggest that translational variance originates from the presence of the regions in which the quantum fluctuations have different masses. The numerical results in table IV and Eqs. (25) and (26) show that the rate at which the VPE changes is not sensitive to the particular shape of the background; but it depends on  $v_0$ . Formally we could add the omission of Eq. (13)

$$\int \frac{dk}{2\pi} \sqrt{k^2 + m_L^2} \frac{d}{dk} \left[ \sqrt{k^2 - v_0} - k \right] \sim \int \frac{dk}{2\pi} \frac{k}{\sqrt{k^2 + m_L^2}} \left[ k - \sqrt{k^2 - v_0} \right]$$

to the energy density to eliminate the (leading) translational variance. The above integration by parts misses a surface term whose divergence is regularized by the Born subtraction in the actual calculation of Eq. (26). We see that translational variance is qualitatively linked to the difference between the densities of states at positive and negative infinity, yet quantitative conclusions are not possible because that difference cannot be explicitly related to the center of the background potential. The picture emerges that shifting the region with the larger mass towards negative infinity removes modes from the spectrum and thus decreases the VPE. On the other hand it is not surprising that the bound state energies are translationally invariant because the bound state wave functions do not reach to spatial infinity.

By shifting the arguments in Eq. (19) we have verified that the proposed numerical approach indeed produces translationally invariant VPEs (actually phase shifts) for the  $\phi^4$  and sine—Gordon solitons. In the present formalism that verification is simple. In contrast, decoupling even and odd parity channels, as required to obtain Eq. (17), distinguishes x=0 and does not leave space for varying the coordinate argument.

Substituting the symmetrized kink-antikink barrier

$$\phi_0(x) = \left[1 + e^{2(x-\bar{x})}\right]^{-1/2} + \left[1 + e^{-2(x+\bar{x})}\right]^{-1/2} - 1$$
(27)

into  $U''(\phi)$  produces a symmetric background that is a variation of a barrier with approximate width  $2\bar{x}$ . The vacuum is characterized by  $m_L = 1$ . Numerically we find

$$\lim_{\bar{x} \to \infty} \left\{ E_{\text{vac}}[U''(\phi_0)] - 2E_{\text{vac}}[V_{\text{SB}}^{(2\bar{x})}] \right\} = -0.340 = 2 \times (-0.170)$$
(28)

which is in the right ball park in comparison with the data in the  $\phi^6$  row of table IV. Unfortunately, it is not clear which value of  $x_s$  in  $V_{\rm SB}^{(2x_s)}$  to use for the subtraction in Eq. (28). For example, it is sensible to define the center of the soliton  $\left[1 + \mathrm{e}^{2(x-\bar{x})}\right]^{-1/2}$  via its classical energy density  $\epsilon(x) = \frac{1}{2}\phi_0'^2 + U(\phi_0)$ :

$$x_s = \frac{\int dx x \epsilon(x)}{\int dx \epsilon(x)} = \bar{x} + \frac{1}{2}$$

and subtract  $V_{\rm SB}^{(2x_s)}$  in Eq. (28). This changes that result to  $-0.239 = 2 \times (-0.120)$ . When attempting to extract the kink VPE from the antikink–kink configuration  $\phi_0(x) = \left[1 + \mathrm{e}^{-2(x-\bar{x})}\right]^{-1/2} + \left[1 + \mathrm{e}^{2(x+\bar{x})}\right]^{-1/2}$ , a well of depth  $v_0$  and width  $2\bar{x}$  is generated yielding a completely different VPE due to the many bound states that emerge for large antikink–kink separation.

## V. CONCLUSION

We have developed a method to compute the VPE for localized configurations in one space dimension. It is based on spectral methods but generalizes previous approaches to configurations that are not amenable to a partial wave decomposition. Being a generalization of the spectral method, the novel approach also naturally inherits the renormalization from the perturbative sector. The proposed method is very efficient: For a given background potential the numerical simulations only take only a few CPU minutes on a standard desktop computer. We solve two uncoupled second order ordinary differential equations, Eq. (7), for the complex valued functions A(x) and B(x) that determine the scattering matrix. An equally simple equation (4) yields the bound state energies. Here we have only considered a single boson field, but taking A(x) and B(x) to be matrix valued straightforwardly generalizes the method to multiple fields and/or fermions. The efficiency can also be established when confronting it with the heavy machinery needed for the heat kernel approach [5, 7] that was earlier used to find the VPE of configurations lacking the symmetries for a partial wave decomposition. We consider the present method at least as efficient as that used in Ref. [11], which is

based on a particular technique to compute functional determinants [19]. Both methods solve a differential equation for single particle energies. Integrating over these energies yields the VPE.

As an application we have considered configurations for which the quantum fluctuations have different masses at positive and negative spatial infinity. Then the background can be interpreted as a modification of a step function potential that interpolates between different vacua. Though the parameterization of the solutions to the stationary wave equation differs on the left and right half lines (joined at the matching point  $x_m$ ) we stress that we always solve the wave equation for the full problem. We have ensured that all results for the VPE (actually for the eigenphase shifts) do not depend on  $x_m$ . We did not explicitly compute the VPE versus another configuration; but the step function potential featured essential when (i) identifying the Born approximation for renormalization and (ii) establishing independence from technical parameters like  $x_m$ .

Though we may freely choose  $x_m$  for computing the scattering matrix, translational invariance with respect to the center of the soliton is lost when the masses of the quantum fluctuations differ at positive and negative spatial infinity. This loss of translational invariance signals that the global vacuum structure is locally relevant. We have also collected numerical and formal evidence that this position dependence is (mainly) due to the differences of the densities of states for scattering modes incident from positive or negative infinity. Even if this was the only cause, the multiple by which the corresponding spatial energy density should be subtracted is not unique leaving a residual position dependence.

In the  $\phi^6$  model the exact no–tadpole renormalization scheme is required. Any additional, though finite, renormalization of the counterterm coefficient is not well defined as the multiplying spatial integral is infinite. However, this is not too surprising as the model is not fully renormalizable.

We wish to extend the present approach in the framework of the interface formalism [20] and use it to investigate domain wall dynamics. This will allow a comparison with the results of Ref. [11]. Also other soliton models in one space dimension can be investigated. For example, the  $\phi^8$  model [21] has solitons within different topological sectors. Comparing their VPE will shed some light on the relevance of quantum corrections to the binding energies of solitons that represent nuclei [22].

### Acknowledgments

Helpful discussions with N. Graham and M. Quandt are gratefully acknowledged. This work is supported in parts by the NRF under grant 77454.

- [1] N. Graham, M. Quandt, H. Weigel, Lect. Notes Phys. 777 (2009) 1.
- N. Graham, R. L. Jaffe, V. Khemani, M. Quandt, M. Scandurra, H. Weigel, Nucl. Phys. B 645 (2002) 49.
- [3] M. A. Lohe, Phys. Rev. D 20 (1979) 3120.
- [4] M. A. Lohe, D. M. O'Brien, Phys. Rev. D 23 (1981) 1771.
- [5] A. Alonso-Izquierdo, J. Mateos Guilarte, Nucl. Phys. B 852 (2011) 696.
- 6] A. Alonso-Izquierdo, J. Mateos Guilarte, Annals Phys. 327 (2012) 2251.
- [7] A. Alonso-Izquierdo, W. Garcia Fuertes, M. A. Gonzalez Leon, J. Mateos Guilarte, Nucl. Phys. B 635 (2002) 525
- [8] E. Elizalde, Lect. Notes Phys. Monogr. **35** (1995) 1.
- [9] E. Elizalde, S. D. Odintsov, A. Romeo, A. A. Bytsenko, S. Zerbini, Zeta regularization techniques with applications, (World Scientific, Singapore, 1994).
- [10] K. Kirsten, AIP Conf. Proc. 484, 106 (1999).
- [11] A. Parnachev, L. G. Yaffe, Phys. Rev. D 62 (2000) 105034.
- [12] K. Kiers, W. van Dijk, J. Math. Phys. 37 (1996) 6033.
- [13] G. Barton, J. Phys. A 18 (1985) 479.
- [14] N. Graham, R. L. Jaffe, M. Quandt, H. Weigel, Annals Phys. 293 (2001) 240.
- [15] J. S. Faulkner, J. Phys. C, 10 (1977) 4661
- [16] A. R. Aguirre, G. Flores-Hidalgo, arXiv:1609.07341 [hep-th].
- [17] R. Rajaraman, Solitons and Instantons, North Holland, 1982
- [18] N. Graham, R. L. Jaffe, Phys. Lett. B **435** (1998) 145.
- [19] S. Coleman, Aspects of Symmetry, Cambridge University Press, 1985.
- [20] N. Graham, R. L. Jaffe, M. Quandt, H. Weigel, Phys. Rev. Lett. 87 (2001) 131601.
- [21] V. A. Gani, V. Lensky, M. A. Lizunova, JHEP 1508 (2015) 147.
- [22] D. T. J. Feist, P. H. C. Lau, N. S. Manton, Phys. Rev. D 87 (2013) 085034.